Design of a disulfide-less, pharmacologically inert, and chemically competent analog of maurocalcine for the efficient transport of impermeant compounds into cells.

Narendra Ram, Norbert Weiss, Isabelle Texier-Nogues, Sonia Aroui, Nicolas Andreotti, Fabienne Pirollet, Michel Ronjat, Jean-Marc Sabatier, Hervé Darbon, Vincent Jacquemond, et al.

DESIGN OF A DISULFIDE-LESS, PHARMACOLOGICALLY-INERT AND CHEMICALLY-COMPETENT ANALOG OF MAUROCALCINE FOR THE EFFICIENT TRANSPORT OF IMPERMEANT COMPOUNDS INTO CELLS

Narendra Ram[1], Norbert Weiss[2], Isabelle Texier-Nogues[3], Sonia Aroui[1], Nicolas Andreotti[4], Fabienne Pirollet[1], Michel Ronjat[1], Jean-Marc Sabatier[4], Hervé Darbon[5], Vincent Jacquemond[2] and Michel De Waard[1*]

Unité Inserm 836, Grenoble Institute of Neuroscience, Research group 3 « Calcium Channels, Functions and Pathologies », Université Joseph Fourier, Site Santé, BP 170, 38042 Grenoble Cedex 09, France[1], Physiologie Intégrative Cellulaire et Moléculaire, Université Claude Bernard Lyon 1, UMR CNRS 5123, 69622 Villeurbanne, France[2], CEA Grenoble/LETI-DTBS, 17 rue des Martyrs, 38054 Grenoble cedex, France[3], ERT62, Université de la Méditérannée – Ambrillia Biopharma, Faculté de Médecine Nord, Marseille Cedex 20, France[4], AFMB CNRS-UMR 6098, Aix-Marseille Universités, Campus de Luminy, 163 Avenue de Luminy, F-13288 Marseille cedex 09, France[5].

Running head: New maurocalcine analog for chemical coupling of cargoes

Address correspondence to: Dr. Michel De Waard, Inserm U836, GIN, UJF, BP 170, 38042 Grenoble Cedex 09, France. Tel.: +33 (0)4 56 52 05 63; E-mail: michel.dewaard@ujf-grenoble.fr

Maurocalcine is a 33-mer peptide initially isolated from the venom of a Tunisian scorpion. It has proved itself valuable as a pharmacological activator of the ryanodine receptor, and has helped the understanding the molecular basis underlying excitation-contraction coupling in skeletal muscles. Because of its positively charged nature, it is also an innovative vector for the cell penetration of various compounds. We report a novel maurocalcine analog with improved properties: (i) the complete loss of pharmacological activity, (ii) preservation of the potent ability to carry cargo molecules into cells, and (iii) with coupling chemistries not affected by the presence of internal cysteine residues of maurocalcine. We did this by replacing the six internal cysteine residues of maurocalcine by isosteric 2-aminobutyric acid residues and by adding an additional N-terminal biotinylated lysine (for a proof of concept analog) or an N-terminal cysteine residue (for a chemically-competent coupling analogue). Additional replacement of a glutamate residue by alanyl at position 12 further improves the potency of these analogues. Coupling to several cargo molecules or nanoparticles are presented to illustrate the cell penetration potency and usefulness of these pharmacologically inactive analogs.

Maurocalcine (MCa) is a highly basic 33-mer peptide isolated from the venom of the scorpion *Scorpio maurus palmatus*. It efficiently binds to the ryanodine receptor in skeletal muscles (RyR1 isoform) (1) and promotes channel opening to promote calcium release from the sarcoplasmic reticulum (SR). This pharmacological effect of MCa can be indirectly monitored through the stimulation it exerts on [^{3}H]-ryanodine binding (2). In muscle fibers, MCa produces a transient loss of voltage control of Ca^{2+} release from RyR1 channels. This effect is due to an alteration of repolarization-induced closure of RyR1 channels, a process normally under the control of voltage-dependent dihydropyridine (DHP)-sensitive calcium channels (3). This function of MCa is due to a partial sequence homology between MCa and a cytoplasmic loop of the DHP-sensitive channel (2). These observations explain why MCa, along with other members of the same family of toxins such as imperatoxin 1A (4), hemicalcin (5), and opicalcin 1 and 2 (6), are useful both for their pharmacological properties and for deciphering fine molecular details of the excitation-contraction coupling process.

Recently, MCa has also proven of interest for its property of efficiently crossing the plasma membrane, either alone or when coupled to a membrane-impermeant cargo protein (2,7). MCa is a highly charged peptide with 12 basic residues out of 33, and a net global positive charge of +8. Most of these residues are on one face of the molecule, the opposite face being mostly hydrophobic in nature. The rich content in basic amino acid residues of MCa is reminiscent of that of all cell penetrating peptides (CPPs) characterized so far (Tat, penetratin and poly-R). Hence, MCa can be classified within an emerging family of toxin CPPs

that have no structural homologies apart from their content in basic residues. Recently, a new toxin, crotamin, has been purified from the venom of a South American snake. It also behaves as a CPP but apparently with a preference for dividing cells (8). The great diversity in CPP sequences observed so far suggests that designing new MCa CPP analogues should be easy. This tolerance in sequence variation is possibly due to the diverse nature of membrane receptors implicated in CPP cell translocation. These receptors nevertheless possess a single point in common: they all appear to interact with CPPs on the basis of electrostatic interactions. On the contrary, the structural characteristics of the interaction between MCa and RyR1 appear far more constrained. A single mutation within MCa, the replacement of an Arg residue by an alanyl, abolishes the pharmacological effect of MCa but has only mild effects on its cell penetration efficacy (9). Nevertheless, segregating the pharmacological properties from the cell penetrating properties proved more complex than expected on the sole basis of amino acid substitutions of MCa (9). This appears to be due to structural imperatives of the molecule since it has four functions to fulfill: first, possess the attributes of a CPP, second, conserve sequence homology with the DHP-sensitive calcium channel, third, bind to RyR1 and fourth, activate this latter channel. Many residues contribute both to the pharmacological effects and the cell penetration properties, namely some basic residues that make the functional segregation difficult with simple amino acid substitutions.

To both circumvent these difficulties and take advantage of the flexibility in structural constraints required for MCa cell penetration, we sought a novel strategy for the design of an MCa analogue that would lose its pharmacological activity while retaining most of its cell penetration efficacy. As determined by ^{1}H-NMR, MCa folds along an inhibitor cystine knot motif with a disulfide bridge pattern of Cys^{3}–Cys^{17}, Cys^{10}–Cys^{21}, and Cys^{16}–Cys^{32}. It contains three β-strands that run from amino acid residues 9–11 (strand 1), 20–23 (strand 2), and 30–33 (strand 3), with β-strands 2 and 3 forming an antiparallel β-sheet (10). In earlier studies on another toxin, maurotoxin (MTX), active on voltage-gated potassium channels, it was found that the disulfide bridges of the peptide play an essential role in the three-dimensional structure of the toxin and thus on its activity (11). We therefore adopted a similar strategy for the design of a novel analogue of MCa in which we replaced all native cysteine residues, engaged in the three disulfide bridges, by isosteric 2-aminobutyric acid residues. The goal was to obtain a structurally-altered analogue displaying a complete loss of pharmacological activity but preserving the positively charged nature of the peptide, a property required for the efficient cell penetration of a CPP. To further validate this analogue, three derivatives were produced that comprise either an N-terminal biotinylated lysine residue with or without an alanyl substitution of Glu^{12}, previously shown to favor cell penetration (9), or an N-terminal cysteine residue for coupling chemistries to various cargoes. This chemical synthesis was accompanied by pharmacological assays, toxicity experiments, and proof of concept that cargo penetration is fully conserved. The data indicate that cysteine replacement within MCa can produce potent cell-penetrating analogues of MCa devoid of pharmacological activity.

Experimental Procedures

Reagents – Streptavidin-Cy5 (Strep-Cy5) was from Amersham Biosciences (USA), dihydroethidium (DHE) from Molecular Probes (USA), and rhodamine- and FITC-conjugated concanavalin A were from AbCys and Sigma, respectively. Doxorubicin was from Alexis Biochemicals (USA). The TK705-amino-(polyethyleneglycol) quantum dots (QD) with surface activated amine groups were purchased from InVitrogen. [^{3}H]-ryanodine was from Perkin-Elmer (USA).

Peptide synthesis - MCa_b was synthesized as previously described (7). MCa_b-Abu, MCa_b-Abu E12A and FITC-Gpep-Cys were purchased from the Department of Pharmaceutical Sciences, University of Ferrara (Italy). Cys-MCa-Abu was synthesized by NeoMPS (France). MTX_b-Abu was assembled by the group of Dr. JM Sabatier (France).

Formation of MCa_b/, MCa_b-Abu/, MCa_b-Abu E12A/, or MTX_b-Abu/Strep-Cy5 complexes – Soluble Strep-Cy5 was mixed with four molar equivalents of MCa_b, MCa_b-Abu, MCa_b-Abu E12A or MTX_b-Abu for 2 hrs at 37°C in the dark in phosphate-buffered saline (PBS, in mM: NaCl 136,

Na_2HPO_4 4.3, KH_2PO_4 1.47, KCl 2.6, $CaCl_2$ 1, $MgCl_2$ 0.5, pH 7.2).

Conjugation of Cys-MCa-Abu to various cargoes – Cys-MCa-Abu was conjugated to a FITC-Gpep-Cys molecule (sequence derived from $G\beta_1$: FITC-beta-AGITSVAFSRSGRLLLAGYDDFN-Abu-NIWDAMKGDRAC-OH) according to the method used by Davidson *et al.* (12). Briefly, an equimolar mixture of Cys-MCa-Abu and FITC-Gpep-Cys was heated to 65°C for 15 min and then incubated at 37°C for 1 hr. The complex was purified by fast protein liquid chromatography.

Cys-MCa-Abu was also conjugated to doxorubicin. Briefly, doxorubicin.HCl (1 mg/ml) was suspended in PBS pH 8.0 and conjugated to Cys-MCa-Abu using succinimidyl-4-(N-maleimidomethyl) cyclohexane-1-carboxylate (Pierce) according to the protocol of Liang et al. (13). Successful coupling was followed by a 16.5% SDS-PAGE and UV detection of the resulting conjugated doxorubicin-linker-Cys-MCa-Abu peptide.

QD were also conjugated to Cys-MCa-Abu. The amino groups of the QD (≈ 100 to 120 functions per particle) were first converted into a maleimide coating as described (14), thereby yielding QD_M. Briefly, QD (1 nmol) were incubated for 4 hrs in the dark at room temperature in PBS in the presence of 4-maleimidobutyric acid *N*-hydrosuccinimide ester (1.8 µmol, in anhydrous dimethylsulfoxide (DMSO)), then purified using NAP-5 columns (Amersham Biosciences). 20 µL of tris-(2-carboxyethyl)phosphine hydrochloride solution 0.5 M was added to 100 nmol of the Cys-MCa-Abu in 80 µL of water for 30 min, and then incubated overnight at room temperature with QD_M in the presence of 1 mM EDTA pH 7.4. Non-reacted maleimide groups were quenched for 20 min by adding 2-mercapthoethanol in excess (500 nmol). The QD_M-Cys-MCa-Abu conjugates were purified using NAP-5 columns (Amersham Biosciences). Surface modifications of QD were detected by 1% agarose gel electrophoresis in a TAE buffer pH 8, and imaged by fluorescence using a 633 nm excitation wavelength and collecting emitted light above 700 nm. The hydrodynamic diameter of the QD_M-Cys-MCa-Abu nanoparticles measured using a Zetasizer Nano (Malvern Instruments) were 25 nm in PBS (20.5 nm for non-modified QD). The QD_M-Cys-MCa-Abu concentration was calculated using 532 nm absorbance measurements (QD molar extinction coefficient $\varepsilon = 2.1 \times 10^6\ M^{-1}\ cm^{-1}$ at 532 nm).

Cell culture – Wild-type Chinese Hamster Ovary (CHO-K1) cells (from ATCC) were maintained at 37°C in 5% CO_2 in F-12K nutrient medium (Invitrogen) supplemented with 10% (v/v) heat-inactivated fetal bovine serum (InVitrogen) and 10,000 units/ml streptomycin and penicillin (Invitrogen). MDA-MB-231 cells from ATCC were grown in Leibovitz L15 medium supplemented with 10% (v/v) heat-inactivated fetal bovine serum and 10,000 units/ml streptomycin and penicillin. Media used for the culture of cerebellar granule neurons was based on Dulbecco's modified Eagle's medium (DMEM, Invitrogen) containing 10 unit/ml penicillin, 10 µg/ml streptomycin, 2 mM L-glutamine, and 10 mM HEPES, 25 mM KCl and 10% fetal bovine serum. Primary cultures were prepared from 6-day-old S/IOPS NMRI mice (Charles River Laboratories), as described previously (15).

Preparation of heavy SR vesicles - Heavy SR vesicles were prepared following the method of Kim *et al.* (16). Protein concentration was measured by the Biuret method.

Isolation and preparation of flexor digitorum brevis muscle fibers – Experiments were performed on single skeletal fibers isolated from the *flexor digitorum brevis* (FDB) muscles from 4- to 8-week old OF1 mice (Charles River Laboratories, France) in accordance with the guidelines of the French Ministry of Agriculture (87/848) and of the European Community (86/609/EEC). Procedures for enzymatic isolation of single fibers and partial insulation of the fibers with silicone grease were as previously described (17,18). In brief, mice were killed by cervical dislocation after halothane (Sigma-Aldrich, France) inhalation before removal of the muscles. Muscles were treated with 2 mg/ml collagenase type I (Sigma-Aldrich) in Tyrode solution for 60 min at 37°C. Single fibers were then isolated by triturating the muscles in the experimental chamber. The major part of a single fiber was electrically insulated with silicone grease (Rhodia Siliconi Italia, Treviolo, Italia) so that whole-cell voltage-clamp could be achieved on a short portion of the fiber extremity. All experiments were performed at room temperature (20-22°C).

Structural analyses of MCa_b, MCa_b-Abu, MCa_b-Abu E12A by circular dichroism – Circular dichroism (CD) spectra were recorded on a Jasco 810 dichrograph using 1 mm-thick quartz cells. Spectra were recorded between 180 and 260 nm at 0.2 nm/min and were averaged from three independent acquisitions. The spectra were corrected for water signal and smoothed by using a third-order least squares polynomial fit.

[^{3}H]-ryanodine binding assay – Heavy SR vesicles (1 mg/ml) were incubated at 37°C for 3 hrs in an assay buffer composed of 5 nM [^{3}H]-ryanodine, 150 mM NaCl, 2 mM EGTA, 2 mM $CaCl_2$ (pCa=5), and 20 mM HEPES, pH 7.4. 1 µM MCa_b, MCa_b-Abu or MCa_b-Abu E12A was added to the assay buffer just prior to the addition of heavy SR vesicles. [^{3}H]-ryanodine bound to heavy SR vesicles was measured by filtration through Whatmann GF/B glass filters followed by three washes with 5 ml of ice-cold washing buffer composed of 150 mM NaCl, 20 mM HEPES, pH 7.4. Filters were then soaked overnight in 10 ml scintillation cocktail (Cybscint, ICN) and bound radioactivity determined by scintillation spectrometry. Non-specific binding was measured in the presence of 20 µM cold ryanodine. Each experiment was performed in triplicate and repeated three times. All data are presented as mean ± S.D.

Fluorescent measurements under voltage-clamp conditions – An RK400 patch-clamp amplifier (BioLogic, France) was used in whole-cell configuration as previously described (18). Voltage-clamp was performed with a microelectrode filled with the intracellular-like solution (in mM: 120 K glutamate, 5 Na_2-ATP, 5 Na_2-phosphocreatine, 5.5 $MgCl_2$, 5 D-glucose, 5 HEPES adjusted to pH 7.2 with KOH). Indo-1 (Molecular Probes, USA) was present in this solution at 0.2 mM for fluorescence measurements under voltage-clamp conditions. The extracellular solution contained (in mM): 140 TEA-methanesulphonate, 2.5 $CaCl_2$, 2 $MgCl_2$, 0.002 tetrodotoxin, 10 HEPES, pH 7.2. The tip of the microelectrode was inserted through the silicon, within the insulated part of the fiber. Membrane depolarizations were applied every 30 s from a holding command potential of -80 mV. For the present set of measurements, the cytoplasm was dialyzed with the microelectrode solution which contained the calcium dye Indo-1 and a given peptide to be tested (200 µM for MCa_b-Abu and MCa_b-Abu E12A, and 100 µM for MCa_b). In order to facilitate intracellular dialysis, the electrode tip was broken within the silicon-insulated portion of the fiber by pushing it back and forth a few times towards the bottom of the chamber. Under these conditions, intracellular equilibration of the solution was awaited for 30 min. Equilibration was followed from the time course of increase of indo-1 fluorescence in the tested portion of the fiber. Indo-1 fluorescence was measured on an inverted Nikon Diaphot epifluorescence microscope equipped with a commercial optical system allowing the simultaneous detection of fluorescence at 405 nm (F_{405}) and 485 nm (F_{485}) by two photomultipliers (IonOptix, Milton, MA) upon 360 nm excitation. Background fluorescence at both emission wavelengths was measured next to each fiber tested and was then subtracted from all measurements. In an earlier study, we showed that 10-100 µM levels of MCa were necessary to affect voltage-activated Ca^{2+} release in intact mammalian skeletal muscle fibers (3). For this reason, and despite the cell penetration properties of MCa and of its derivatives, it is easier and less costly to apply these compounds intracellularly through the voltage-clamp electrode rather than in the extracellular medium.

Calibration of the Indo-1 response and $[Ca^{2+}]_{intra}$ calculation – The standard ratio method was used with the parameters: $R = F_{405} / F_{485}$, with R_{min}, R_{max}, K_D and β having their usual definitions. Results were either expressed in terms of Indo-1 percent saturation or in actual free calcium concentration (18,19). *In vivo* values for R_{min}, R_{max} and β were measured using procedures previously described (17). No correction was made for Indo-1 Ca^{2+} binding and dissociation kinetics.

MTT assay - Primary cultures of cerebellar granule neurons were seeded into 96 well micro plates at a density of approximately 8×10^4 cells/well. After 4 days of culture, the cells were incubated for 24 hrs at 37°C with 10 µM MCa_b, MCa_b-Abu, Cys-MCa-Abu or MCa_b E12A-Abu. Control wells containing cell culture medium alone or with cells, both without peptide addition, were included in each experiment. The cells were then incubated with 3-(4, 5-dimethylthiazol-2-yl)-2, 5-diphenyl-tetrazolium bromide (MTT) for 30 min. Conversion of MTT into purple colored MTT formazan by the living cells indicates the degree of

cell viability. The crystals were dissolved in DMSO and the optical density was measured at 540 nm using a microplate reader (Biotek ELx-800, Mandel Scientific Inc.) for quantification of cell viability. All assays were run in triplicate.

Flow cytometry – MCa_b/, MCa_b-Abu/, MCa_b-Abu E12A or MTX_b-Abu/Strep-Cy5 complexes were incubated for 2 hrs with CHO cells to allow cell penetration. Control condition was represented by an incubation of cells with Strep-Cy5 alone. The cells were then washed twice with PBS to remove the excess extracellular complexes. Next, the cells were treated with 1 mg/ml trypsin (Invitrogen) for 10 min at 37°C to remove remaining membrane-associated extracellular cell surface-bound complexes. Cell suspension was centrifuged at 500 g and resuspended in PBS. Flow cytometry analyses were performed with live cells using a Becton Dickinson FACSCalibur flow cytometer (BD Biosciences). Data were obtained and analyzed using CellQuest software (BD Biosciences). Live cells were gated by forward/side scattering from a total of 10,000 events. Mean fluorescence values were determined from Gaussian fits of the resulting histograms and plotted as a function of complex concentration. Mean values of intracellular fluorescence for Strep-Cy5 alone incubation (less than 1% of the fluorescence observed for the lowest concentration of any of the various MCa / Strep-Cy5 complexes) were also subtracted.

Analysis of the subcellular localization of various MCa / or MTX/ cargo complexes by confocal microscopy – For Strep-Cy5 complexes, 4 µM of MCa_b, MCa_b-Abu, MCa_b-Abu E12A or MTX_b-Abu were coupled to 1 µM Strep-Cy5 as described above. CHO cells were incubated with the resulting complexes for 2 hrs, and then washed with DMEM alone. Immediately after washing, the nucleus was stained with 1 µg/ml DHE for 20 min, and then washed again with DMEM. After this step, the plasma membrane was stained with 5 µg/ml of FITC-conjugated concanavalin A for 3 min. Cells were washed once more, but with PBS. For the FITC-Gpep-Cys-Cys-MCa-Abu complex, 1 µM of the conjugate was incubated with CHO cells for 2 hrs, the plasma membrane stained with 5 µg/ml of rhodamine-conjugated concanavalin A. For the QD_M-Cys-MCa-Abu complex, 50 nM of the complex was incubated with CHO cells for 2 hrs, and the nuclei stained with 1 µg/ml DHE for 20 min. For the doxorubicin-linker-Cys-MCa-Abu complex, 3 µM of the conjugate was incubated with MDA-MB-231 for 2 hrs, followed by staining of the plasma membrane with 5 µg/ml of FITC-conjugated concanavalin A for 3 min. In all experiments, live cells were immediately analyzed by confocal laser scanning microscopy using a Leica TCS-SP2. Alexafluor-488 (excitation at 488 nm), rhodamine and doxorubicin (excitation at 543 nm), or Cy5 and QD_M (excitation at 642 nm) were sequentially excited and emission fluorescence collected in z-confocal planes of 10-15 nm steps. Images were merged in Adobe Photoshop 7.0.

RESULTS

Synthesis of disulphide-less analogs of MCa - Fig. 1A illustrates the three-dimensional solution structure of MCa with three disulphide bridges. The aim of this study was to design a MCa analog for which convenient chemical coupling could be performed by using an N-terminal additional cysteine residue. As shown, MCa already contains six cysteine residues that contribute to the folding of the peptide to form an inhibitor cysteine knot motif. Adding an additional cysteine residue at the N-terminus may significantly change the normal folding of the peptide and the classical disulfide bridge arrangement (C_1-C_4, C_2-C_5, and C_3-C_6) in an unpredicted manner. In turn, this could significantly affect the pharmacological activity and cell-penetration properties of the resulting molecule(s). To facilitate chemical coupling strategies of MCa to cargo molecules, we investigated the requirement of disulfide bridges on MCa's pharmacology and cell penetration properties. Several analogs were synthesized, each with an N-terminal biotinylated lysine for easy coupling to fluorescent streptavidin molecules (our reporter cargo for this study): MCa_b, intact with the native disulfide bridges, MCa_b–Abu in which we replaced all internal cysteine residues by isosteric 2-aminobutyric acid (Abu, Fig. 1B), and MCa_b-Abu E12A, an analog of MCa_b-Abu in which Glu^{12} was replaced by alanyl, a substitution known to improve cell penetration efficacy of MCa_b (9) (Fig. 1C). We would expect that removing the disulfide bridges of MCa might affect its pharmacology more than its cell penetration properties for two reasons. First, disulfide bridge patterns are known to contribute to the pharmacological activity of

toxins (20,21). Second, the structural requirements for the pharmacological activity of MCa were shown to be more stringent than those required for cell penetration as probed by alanine scanning of MCa (9). Finally, we synthesized MTX_b-Abu, a biotinylated version of MTX that has no cell penetrating properties on its own and that acts on voltage-dependent potassium channels (Fig. 1D). This peptide, in which we also replaced six internal cysteine residues by Abu derivatives, as for the MCa_b-Abu peptide, was used as a negative control in cell penetration experiments.

Removing disulfide bridges in MCa disrupts the secondary structure of the peptide – Circular dichroism analyses were performed for MCa_b, MCa_b-Abu, and MCa_b-Abu E12A (Fig. 2). As shown, the spectra for MCa_b-Abu and MCa_b-Abu E12A differed significantly from MCa_b indicating the alteration of secondary structures of the peptides. These observations are coherent with a role of disulfide brides in the acquisition/stabilization of secondary structures of toxins (11). These data clearly indicate that blocking disulfide bridge formation in MCa is a successful strategy to alter the structure of MCa.

Cysteine replacement by Abu derivatives produces pharmacologically-inert MCa analogues – MCa is known to bind to RyR1 from skeletal muscles (2). Upon binding, it modifies the conformation of this intracellular calcium channel in such a way that it favours binding of [^{3}H]-ryanodine to its receptor, probably by converting low affinity binding sites to high affinity one. The effect of 1 µM MCa_b on [^{3}H]-ryanodine binding to sarcoplasmic reticulum (SR) containing RyR1 was confirmed in this study (Fig. 3). An average stimulation in binding of 59.7-fold was measured (n=3). The value of this stimulation depends upon the basal level of binding and can occasionally be lower, down to 7-fold (not shown). Importantly, the two analogs in which the cysteine residues were replaced by Abu derivatives, MCa_b-Abu and MCa_b-Abu E12A, had no significant effect on [^{3}H]-ryanodine binding indicating that the structural impact of these substitutions fully blocked the effect of MCa on RyR1. Slight reductions in [^{3}H]-ryanodine binding were observed although these effects were not significant. Higher concentrations of these two analogs were also without effect (not shown). The E12A substituted analogue thus proved no better than MCa_b-Abu in spite of the fact that a similar mutation in the folded MCa has higher affinity for RyR1 (9).

We also investigated the effect of these analogs on Ca^{2+} homeostasis in muscles fibers. The effects of the three peptides MCa_b, MCa_b-Abu and MCa_b-Abu E12A were tested on the free Ca^{2+} transients elicited by voltage-clamp depolarizations in single skeletal muscle fibers from mouse. Fig. 4A shows representative Indo-1 saturation traces obtained in response to pulses from -80 mV to +10 mV of 5, 10, 20 and 50 ms duration in (from top to bottom) a control fiber, a fiber dialyzed with 100 µM MCa_b, a fiber dialyzed with 200 µM MCa_b-Abu or a fiber dialyzed with 200 µM MCa_b-Abu E12A, respectively. These high concentrations of peptides were chosen to ensure that effective intracellular levels could be reached after equilibration (see Methods). As previously described (3), MCa_b produced a remarkable change in the time course of the Ca^{2+} transients: it prevented membrane repolarization-induced complete turn off of SR Ca^{2+} release, resulting in a prolonged elevation of the cytoplasmic [Ca^{2+}] after the end of the pulses. This was obviously not the case in the two fibers treated respectively with MCa_b-Abu and MCa_b-Abu E12A, for which the Ca^{2+} transients yielded properties very similar to the ones of the control fiber. Corresponding mean values for the peak $\Delta[Ca^{2+}]$ during the pulse, and the final $\Delta[Ca^{2+}]$ at the time of the end of the record, are presented in Fig. 4B,C. For instance, MCa_b produced a mean final $\Delta[Ca^{2+}]$ value of 0.164 ± 0.032 (n=4) following a pulse of 20 ms, whereas MCa_b-Abu and MCa_b-Abu E12A produced only values of 0.019 ± 0.009 (n=9) and 0.016 ± 0.008 (n=11), respectively, compared to 0.017 ± 0.007 (n=10) for the control condition. There was thus no significant difference in the values for the peak $\Delta[Ca^{2+}]$, and the final $\Delta[Ca^{2+}]$ between control fibers and fibers treated with either MCa_b-Abu or MCa_b-Abu E12A clearly demonstrating a complete loss of MCa-induced activity on SR Ca^{2+} release for these two compounds. The effect of MCa likely results from competition with a physiological interaction between the DHP receptors and RyR1 (3) explaining why such high concentrations are required. We conclude that replacement of the cysteine in MCa by Abu derivatives produces non-folded and pharmacologically-inert analogs.

Conserved cell penetration properties of disulfide-less MCa analogues – Biotinylated MCa, MCa_b, favours the efficient penetration of fluorescently-labelled streptavidine (Strep) (7,9,22), through macropinocytosis (23). The cell penetration of MCa_b/Strep complexes involves one or multiple steps of attachment to the membrane through binding to cell surface glycosaminoglycans and negatively charged lipids. The complex can be found predominantly in endosomes, leading to a punctate cytoplasmic distribution, a pattern that is supposedly linked to the nature of the cargo rather than the vector itself. Here, we investigated whether the disulfide-less analogues of MCa_b were capable of carrying Strep-Cy5 into CHO cells (Fig. 5A). As shown, 1 µM of Strep-Cy5 alone is unable to enter CHO cells. This was true for 100% of the cells examined by confocal microscopy (n=200). However, when coupled to either MCa_b, MCa_b-Abu or MCa_b-Abu E12A in a 4 to 1 ratio and incubated for 2 hrs with living CHO cells, the resulting complexes gave punctate staining. Here again, 100% of the cells were positively stained by Strep-Cy5 (n=200 for each condition). This punctate staining is an indication of endosomal distribution further confirming that it may be linked to the nature of the cargo rather than the vector, since similar distributions are observed for the MCa analogs despite the structural changes in the vector. In contrast, no cell penetration of Strep-Cy5 was observed in CHO cells using a biotinylated analogue of MTX, MTX_b-Abu, a voltage-gated K^+ channel blocker (Fig. 5B; 0% of n=200 cells examined by confocal microscopy). This indicates that MCa_b-Abu is unlikely to penetrate non-specifically into cells owing to its amphipatic nature.

In order to obtain half-maximal Penetration Concentration values (PC_{50}) and the extent of total penetration of the complex, quantification of cell penetration by fluorescence activated cell sorting (FACS) was performed. Quantification is a way to distinguish the cell penetration efficacies of various MCa analogs (9) or of various cell lines (23). As shown in Fig. 6, after 2 hrs incubation, both MCa_b-Abu and MCa_b-Abu E12A analogs were less effective than MCa_b since the total Strep-Cy5 fluorescence entering CHO cells at maximally effective concentration of the peptides (10 µM) was reduced on average by 28% and 59% for MCa_b-Abu E12A and MCa_b-Abu, respectively (Fig. 6). It is of interest that the E12A mutant was more effective than the analog without mutation. A similar observation was made with the folded version of this mutation (9). This effect is most likely due to an increase in the basic content of the molecule. With regard to PC_{50} values, only slight reductions in the efficacies of the analogs were observed. In these experiments, we measured PC_{50} values of 669 ± 27 nM for MCa_b/Strep-Cy5 (n=3), 910 ± 51 nM for MCa_b-Abu/Strep-Cy5 (n=3) and 1042 ± 89 nM for MCa_b-Abu E12A/Strep-Cy5 (n=3). Therefore, in the case of disulfide-less analogs, maximal cell penetration of Strep-Cy5 could be obtained by only using slightly increased peptide concentrations.

Adding an N-terminal cysteine residue to a disulfide-less MCa analog produces a chemically-competent peptide for the cell penetration of various cargoes – Although the use of Strep brings proof of concept, it remains a useless cargo for many biological applications, especially if it concentrates into endosomes. We therefore produced a novel disulfide-less analogue of MCa in which we simply replaced the N-terminal biotinylated lysine by a cysteine residue in order to make various chemical coupling strategies possible (Cys-MCa-Abu whose sequence is shown in Fig. 7A). Next, this peptide was coupled to various cargoes using several chemistries and investigated for its ability to enter cells (Fig. 7B-D). Cys-MCa-Abu was first coupled to a FITC fluorescent peptide containing a C-terminal cysteine residue. The coupling consisted in favoring the formation of a disulfide bridge among the two peptides. At 1 µM, this complex entered CHO cells (100% of the cells by confocal microscopy, n=200) whereas incubation of CHO cells with 1 µM FITC-labeled peptide alone resulted in no cell penetration (Fig. 7B; 0% of n=200 cells observed). The FITC-peptide complex stained diffusely the cells indicating that it reached both the cytoplasm and the nucleus either through direct plasma membrane translocation or through endosomal escape. Since the Strep and FITC complexes distribute differently in the cell, it appears that the cargo rather than the vector determines the cell distribution. Cys-MCa-Abu was also coupled to doxorubicin, an anti-tumor drug, which penetrates into MDA-MB-231 cells by itself, and concentrates in nuclei where it acts on DNA replication. The chemical coupling was performed

using a cross-linker, allowing a directional coupling with the unique amino group of doxorubicin and the SH function of the cysteine residue of Cys-MCa-Abu. As shown, incubation of MDA-MB-231 cells with either 3 μM doxorubicin or doxorubicin-linker-Cys-MCa-Abu resulted in significantly different cell distributions (Fig. 7C). Covalent linkage of doxorubicin with Cys-MCa-Abu produced a marked cytoplasmic localization, also diffuse, in marked contrast to the predominantly nuclear distribution of doxorubicin. In 96% of the cells examined (n=200), the coupling to Cys-MCa-Abu resulted in a cytoplasmic distribution of doxorubicin. Finally, near-infrared emitting quantum dots from Invitrogen, with amine surfaces, were linked to Cys-MCa-Abu using maleimide chemistry. Maleimide was added to QD yielding QD_M, that could further be linked to the SH function of the Cys residue of Cys-MCa-Abu. Incubation of 50 nM of QD_M-Cys-MCa-Abu with CHO cells resulted in cell penetration with a diffuse distribution in both the cytoplasm and the nucleus (Fig. 7D; 100% of cells observed; n=200). No penetration was observed with QD_M incubation alone (0% of cells, n=200). The rather efficient penetration observed with such a low concentration of QD_M-Cys-MCa-Abu might be explained by the high potential of Cys-MCa-Abu grafting at the surface of QD_M (about 100 to 120 maleimide converted functions at the surface of a single QD).

Cell toxicity of MCa analogues – To be considered as good cell penetrating vectors, peptides must have limited cell toxicity. We investigated cerebellar granule cell survival after incubation with 10 μM of free vector peptide for 24 hrs (Fig. 8). This cell system is generally used for the evaluation of neuronal survival. It is more stringent than the use of cell lines that are more resistant to toxic agents. The conditions used in this study were deliberately extreme considering the conditions required for the cell penetration of our vectors. First, incubation times in the range of an hour are largely sufficient; second, cell penetration is observed at lower concentrations than 10 μM; and third, we have evidence suggesting that intracellular concentrations of cell penetrating peptides increase markedly when cells are incubated with the vector alone rather than in complex with the cargo. Nevertheless, the experimental conditions used here indicate that only one of the analog had a significant effect on neuronal survival (MCa_b-Abu, mean survival of 74.3 ± 4.9%, n=6), whereas all other analogs were without significant effects despite of the conditions used here (n=6 for each condition).

CONCLUDING REMARKS

By simple substitution of the six cysteine residues of MCa, we have produced a series of analogs that are devoid of secondary structure and therefore of pharmacological activity. These analogs nevertheless possess cell-penetrating properties that are closely related to those established for native MCa. This finding indicates that the proper folding of MCa is not essential for the membrane translocation. Similarly, the spatial separation of a basic face and a hydrophobic face of MCa seems of little importance for cell penetration. It cannot be excluded however that during the translocation process itself, when the peptide interacts with negatively charged lipids, it may adopt a conformation close to that of native MCa. The observation that MTX_b-Abu, used as a negative control, does not penetrate cells indicates that MCa-Abu does not act as a detergent by means of its amphipathic nature. Slight increase in effective concentrations or reductions in total transport capacities of these analogs barely counterbalance the benefits of the loss of pharmacological effects or the ability to graft an extra-N-terminal cysteine residue to the sequence for versatile cargo coupling strategies. Our results further indicate that the Cys-MCa-Abu vector is valuable for the cell delivery of a variety of cargoes. The cytoplasmic localization of the delivered cargoes using this vector should be invaluable for many biological applications for which targeting to this compartment are an absolute requirement. For future applications, it might be recommended to assess the cell toxicity of the vector/cargo complexes of interest in the conditions of the application. The benefits of all cell penetrating peptides undoubtedly lie in the value of penetration/toxicity concentration ratio of the formed complexes, a value that needs to be determined for each application.

REFERENCES

1. Altafaj, X., Cheng, W., Esteve, E., Urbani, J., Grunwald, D., Sabatier, J. M., Coronado, R., De Waard, M., and Ronjat, M. (2005) *J Biol Chem* **280**, 4013-4016
2. Esteve, E., Smida-Rezgui, S., Sarkozi, S., Szegedi, C., Regaya, I., Chen, L., Altafaj, X., Rochat, H., Allen, P., Pessah, I. N., Marty, I., Sabatier, J. M., Jona, I., De Waard, M., and Ronjat, M. (2003) *J Biol Chem* **278**, 37822-37831
3. Pouvreau, S., Csernoch, L., Allard, B., Sabatier, J. M., De Waard, M., Ronjat, M., and Jacquemond, V. (2006) *Biophys J* **91**, 2206-2215
4. el-Hayek, R., Lokuta, A. J., Arevalo, C., and Valdivia, H. H. (1995) *J Biol Chem* **270**, 28696-28704
5. Shahbazzadeh, D., Srairi-Abid, N., Feng, W., Ram, N., Borchani, L., Ronjat, M., Akbari, A., Pessah, I. N., De Waard, M., and El Ayeb, M. (2007) *Biochem J* **404**, 89-96
6. Zhu, S., Darbon, H., Dyason, K., Verdonck, F., and Tytgat, J. (2003) *Faseb J* **17**, 1765-1767
7. Boisseau, S., Mabrouk, K., Ram, N., Garmy, N., Collin, V., Tadmouri, A., Mikati, M., Sabatier, J. M., Ronjat, M., Fantini, J., and De Waard, M. (2006) *Biochim Biophys Acta* **1758**, 308-319
8. Nascimento, F. D., Hayashi, M. A., Kerkis, A., Oliveira, V., Oliveira, E. B., Radis-Baptista, G., Nader, H. B., Yamane, T., Tersariol, I. L., and Kerkis, I. (2007) *J Biol Chem* **282**, 21349-21360
9. Mabrouk, K., Ram, N., Boisseau, S., Strappazzon, F., Rehaim, A., Sadoul, R., Darbon, H., Ronjat, M., and De Waard, M. (2007) *Biochim Biophys Acta* **1768**, 2528-2540
10. Mosbah, A., Kharrat, R., Fajloun, Z., Renisio, J. G., Blanc, E., Sabatier, J. M., El Ayeb, M., and Darbon, H. (2000) *Proteins* **40**, 436-442
11. di Luccio, E., Matavel, A., Opi, S., Regaya, I., Sandoz, G., M'Barek, S., Carlier, E., Esteve, E., Carrega, L., Fajloun, Z., Rochat, H., Loret, E., de Waard, M., and Sabatier, J. M. (2002) *Biochem J* **361**, 409-416
12. Davidson, T. J., Harel, S., Arboleda, V. A., Prunell, G. F., Shelanski, M. L., Greene, L. A., and Troy, C. M. (2004) *J Neurosci* **24**, 10040-10046
13. Liang, J. F., and Yang, V. C. (2005) *Bioorg Med Chem Lett* **15**, 5071-5075
14. Cai, W., Shin, D. W., Chen, K., Gheysens, O., Cao, Q., Wang, S. X., Gambhir, S. S., and Chen, X. (2006) *Nano Lett* **6**, 669-676
15. Gallo, V., Kingsbury, A., Balazs, R., and Jorgensen, O. S. (1987) *J Neurosci* **7**, 2203-2213
16. Kim, D. H., Ohnishi, S. T., and Ikemoto, N. (1983) *J Biol Chem* **258**, 9662-9668
17. Collet, C., Allard, B., Tourneur, Y., and Jacquemond, V. (1999) *J Physiol* **520 Pt 2**, 417-429
18. Jacquemond, V. (1997) *Biophys J* **73**, 920-928
19. Csernoch, L., Bernengo, J. C., Szentesi, P., and Jacquemond, V. (1998) *Biophys J* **75**, 957-967
20. Fajloun, Z., Ferrat, G., Carlier, E., Fathallah, M., Lecomte, C., Sandoz, G., di Luccio, E., Mabrouk, K., Legros, C., Darbon, H., Rochat, H., Sabatier, J. M., and De Waard, M. (2000) *J Biol Chem* **275**, 13605-13612
21. Fajloun, Z., Mosbah, A., Carlier, E., Mansuelle, P., Sandoz, G., Fathallah, M., di Luccio, E., Devaux, C., Rochat, H., Darbon, H., De Waard, M., and Sabatier, J. M. (2000) *J Biol Chem* **275**, 39394-39402
22. Esteve, E., Mabrouk, K., Dupuis, A., Smida-Rezgui, S., Altafaj, X., Grunwald, D., Platel, J. C., Andreotti, N., Marty, I., Sabatier, J. M., Ronjat, M., and De Waard, M. (2005) *J Biol Chem* **280**, 12833-12839
23. Ram, N., Aroui, S., Jaumain, E., Sadoul, R., Mabrouk, K., Ronjat, M., Lortat-Jacob, H., De Waard, M. (submitted)

FOOTNOTES

We thank the team of Pr. Rémy Sadoul for help with cerebellar granule cell cultures. We also thank Dr. Jonathan Coles for critical reading of the manuscript. We acknowledge financial support from Inserm and the Fond de Valorisation of the CEA. Narendra Ram is a fellow of the Région Rhône-Alpes and is supported by an Emergence grant to M.D.W.

*The abbreviations used are: CD, Circular Dichroism; CHO, Chinese Hamster Ovary cells; CPP, Cell Penetrating Peptide; DHE, dihydroethidium; DHP: Dihydropyridine; DMSP, Dimethylsulfoxide; HEPES, 4-(2-hydroxyethyl)-1-piperazineethanesulfonic acid; FACS, Fluorescence Activated Cell Sorter; FDB, Flexor Digitorum Brevis; MCa, maurocalcine; PBS, Phosphate Buffer Saline; PEG, Polyethylene glycol; QD, Quantum Dot; RyR1, Ryanodine Receptor type I; SD, Standard Deviation; SR, Sarcoplasmic Reticulum; Strep-Cy5, Streptavidin-cyanine5.

FIGURE LEGENDS

Fig. 1. MCa analogues, MCa_b-Abu and MCa_b-Abu E12A. *A*. Ribbon representation of the 3D solution structure of MCa illustrating the positions of the three disulfide bridges C_1-C_4, C_2-C_5 and C_3-C_6. S-S bonds are shown in blue. The positions of positively charged lysines, essential for cell penetration, are shown in red. *B*. Differences in side chain between cysteine residues and 2-aminobutyric acid (Abu) used for substitution of all cysteine residues in MCa amino acid sequence. *C*. Amino acid sequences of three different MCa analogs used in this study. A fourth analog is shown in Fig. 7*A*. *D*. Amino acid sequence of MTX_b-Abu, an analog of MTX in which all cysteine residues are replaced by Abu, and an extra biotinylated lysine residue added at the N-terminus. Note that MTX contains six basic amino acid residues in its sequence.

Fig. 2. Determination of the secondary structures of MCa_b, MCa_b-Abu and MCa_b-Abu E12A by circular dichroism. Each spectrum presented is the mean of three independent acquisitions taken at a concentration of 50 µM in pure water at 20°C.

Fig. 3. Effect of 1 µM MCa_b, MCa_b-Abu or MCa_b-Abu E12A on [^{3}H]-ryanodine binding onto heavy SR vesicles. Specific [^{3}H]-ryanodine binding was measured as described under *Materials and Methods*. Control binding has been performed in the absence of MCa analog. ***, $p \leq 0.01$. Note the loss of effect upon cysteine replacement by Abu derivatives. The experiment was repeated three times with similar results.

Fig. 4. Effects of MCa_b, MCa_b-Abu and MCa_b-Abu E12A on voltage-activated sarcoplasmic reticulum Ca^{2+} release. *A*. Indo-1 Ca^{2+} records in response to membrane depolarizations of increasing duration in a control fiber and in fibers dialyzed, respectively, with MCa_b (100 µM), MCa_b-Abu (200 µM) and MCa_b-Abu E12A (200 µM). *B, C*. Corresponding mean values for peak $\Delta[Ca^{2+}]$, and final $\Delta[Ca^{2+}]$ at the end of the record in control fibers (n=11) and in fibers dialyzed with either MCa_b (n=3), MCa_b-Abu (n=10) or MCa_b-Abu E12A (n=3). Note the loss of pharmacological consequences of replacing cysteine by Abu derivatives.

Fig. 5. Distribution of MCa_b/, MCa_b-Abu/ and MCa_b-Abu E12A/Strep-Cy5 in CHO cells. *A*. Confocal images showing the cell penetration of Strep-Cy5 (2 hrs incubation) in the absence or presence of 4 µM MCa_b, MCa_b-Abu or MCa_b-Abu E12A in CHO cells. Colors: blue (Strep-Cy5), red (nuclei, DHE) and green (plasma membrane, concanavalin A). Note the lack of differences in cell distribution between Strep-Cy5 and the MCa analogues used. The punctate distribution is linked to the use of streptavidin as cargo.

Scale bars: 10 µm. *B*. Confocal image of CHO cells showing that 4 µM MTX_b-Abu is unable to deliver Strep-Cy5 inside cells (2 hrs incubation). Color code as in *A*. Scale bar: 15 µm.

Fig. 6. Mean cell fluorescence intensities (MFI) as a function of the concentration of cell penetrating complexes for each MCa analog. Indicated concentrations are for Strep-Cy5 (10 nM to 2.5 µM). The ratio MCa analog / Strep-Cy5 was 4/1. Data were fitted by a sigmoid equation of the type $MFI = MFI_{max} / (1 + \exp(-(x-PC_{50})/b))$ where MFI_{max} = 180 ± 6 a.u. (MCa_b), 73 ± 4 a.u. (MCa_b-Abu) and 129 ± 8 a.u. (MCa_b-Abu E12A), b = 200 ± 18 (MCa_b), 301 ± 38 (MCa_b-Abu) and 344 ± 64 (MCa_b-Abu E12A), and half-penetration concentration values PC_{50} = 669 ± 27 nM (MCa_b), 910 ± 51 nM (MCa_b-Abu) and 1042 ± 89 nM (MCa_b-Abu E12A). a.u.: arbitrary units. The MFI values are obtained from a fit of the FACS histograms (n=10,000 events in each case). Representative example of n=3 experiments. Experiments could not be averaged because the different photomultiplier settings were not calibrated.

Fig. 7. Design of a cell-penetrating analog for the efficient coupling and delivery of a variety of cargoes. *A*. primary amino acid sequence of the Cys-MCa-Abu analog. This analogue is identical to MCa_b-Abu except that the N-terminal K(biot) has been replaced by an N-terminal cysteine residue. *B*. Cell penetration of FITC-Gpep-Cys when covalently linked to Cys-MCa-Abu (right panel, 1 µM concentration, 2 hrs incubation with CHO cells). No penetration is observed for 1 µM FITC-Gpep-Cys alone (left panel). Code colors: red, concanavalin-A-rhodamine, and green, FITC label. *C*. Cell penetration of 3 µM doxorubicin or the covalently linked complex, doxorubicin-linker-Cys-MCa-Abu, in MDA-MB-231 cells. Note that doxorubicin alone goes to the nucleus (red, left panel), whereas coupled to Cys-MCa-Abu it concentrates in the cytoplasm. Green: concanavalin-A-FITC for plasma membrane staining. *D*. Cell penetration of 50 nM quantum dots (QD) alone (left panel) or coupled after maleimide modification of QDs to Cys-MCa-Abu in CHO cells (right panel). Code colors: red, nuclei (DHE) and blue, QDs. From *B* to *D*, note the diffuse cytoplasmic staining of the cargoes when coupled to Cys-MCa-Abu.

Fig. 8. Neuronal toxicity of MCa analogues. Neuronal survival after 24 hrs incubation with 10 µM of each MCa analogue was assessed with the MTT assay. No significant differences in neuronal survival were observed between the analogues. ***, survival affected with mean + 3 S.D. < 100%. Average of 6 data points.

A

MCa

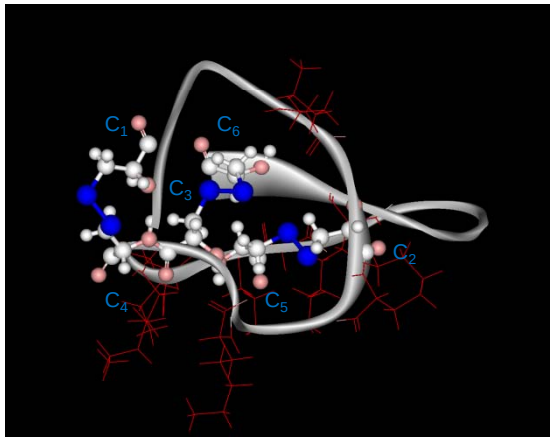

GDC$_1$LPHLKLC$_2$KENKDC$_3$C$_4$SKKC$_5$KRRGTNIEKRC$_6$R

B

Cysteine (C)

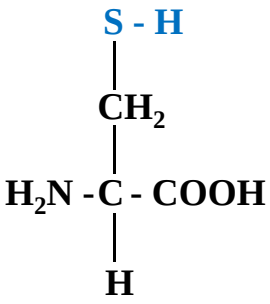

2-Aminobutyric acid (Abu)

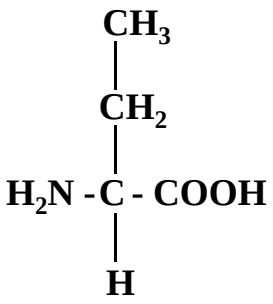

C

MCa$_b$	K(biot) –GDC$_1$LPHLKLC$_2$KENKDC$_3$C$_4$SKKC$_5$KRRGTNIEKRC$_6$R
MCa$_b$-Abu	K(biot) -GDAbuLPHLKLAbuKENKDAbuAbuSKKAbuKRRGTNIEKRAbuR
MCa$_b$-Abu E12A	K(biot) -GDAbuLPHLKLAbuKANKDAbuAbuSKKAbuKRRGTNIEKRAbuR

D

MTX$_b$-Abu	K(biot) -VSAbuTGSKDAbuYAPAbuRKQTGAbuPNAKAbuINKSAbuKAbuYGAbu

Figure 1 – Ram et al.

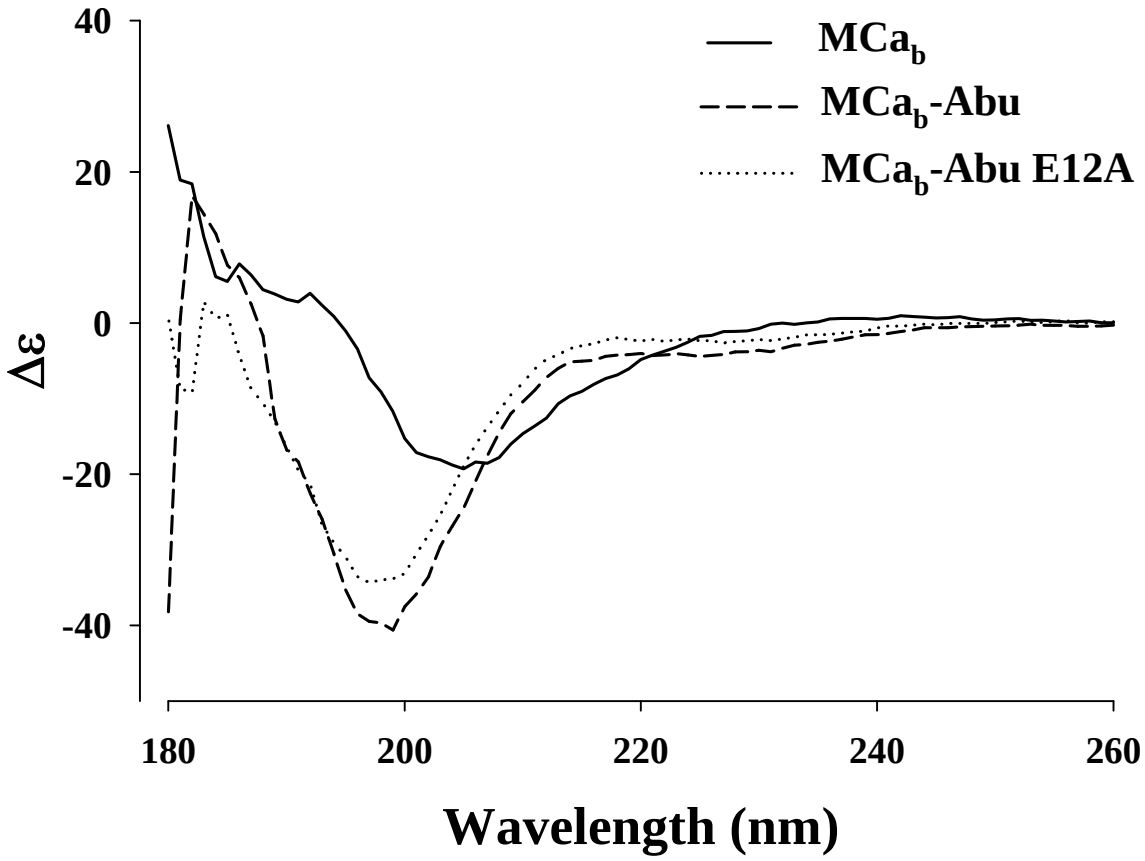

Figure 2 - Ram et al.

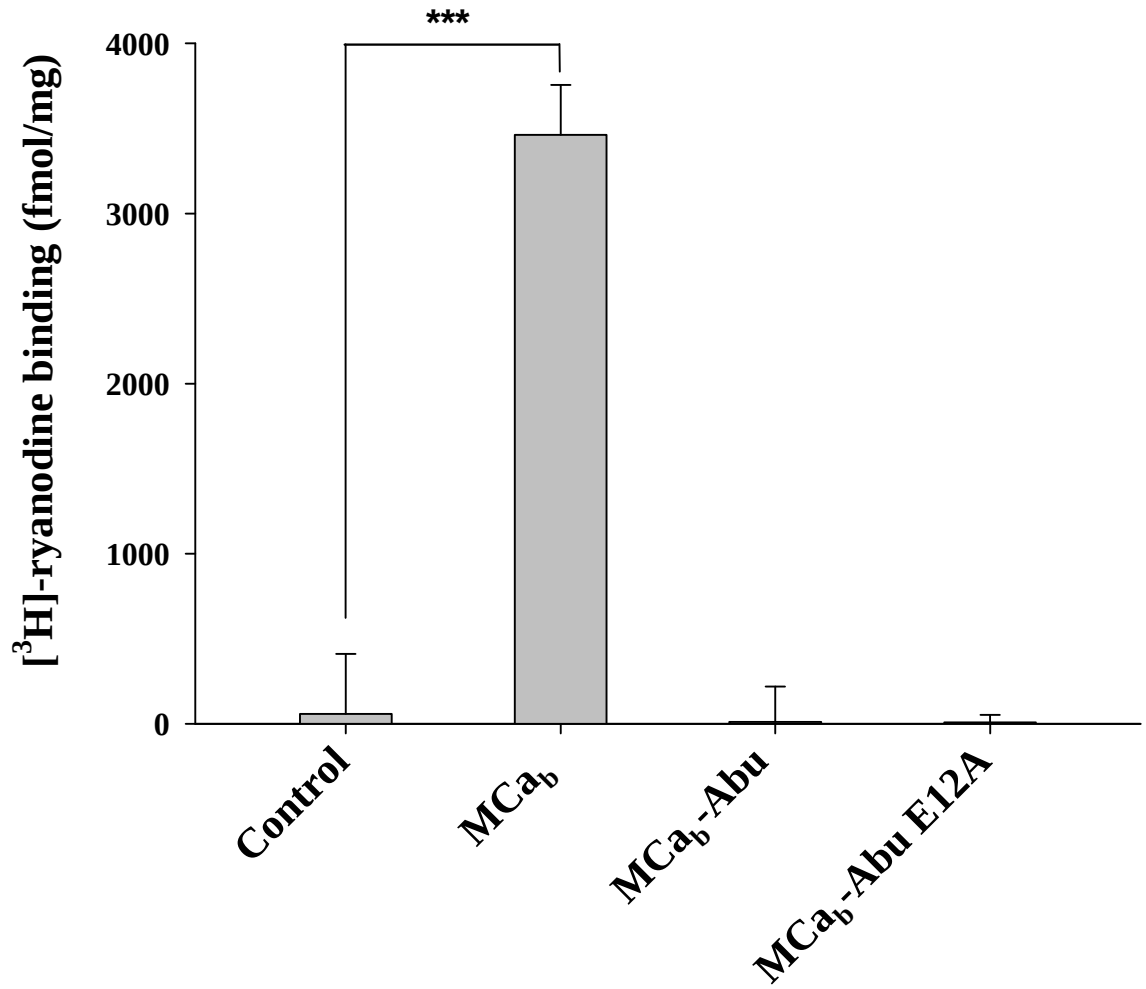

Figure 3 - Ram et al.

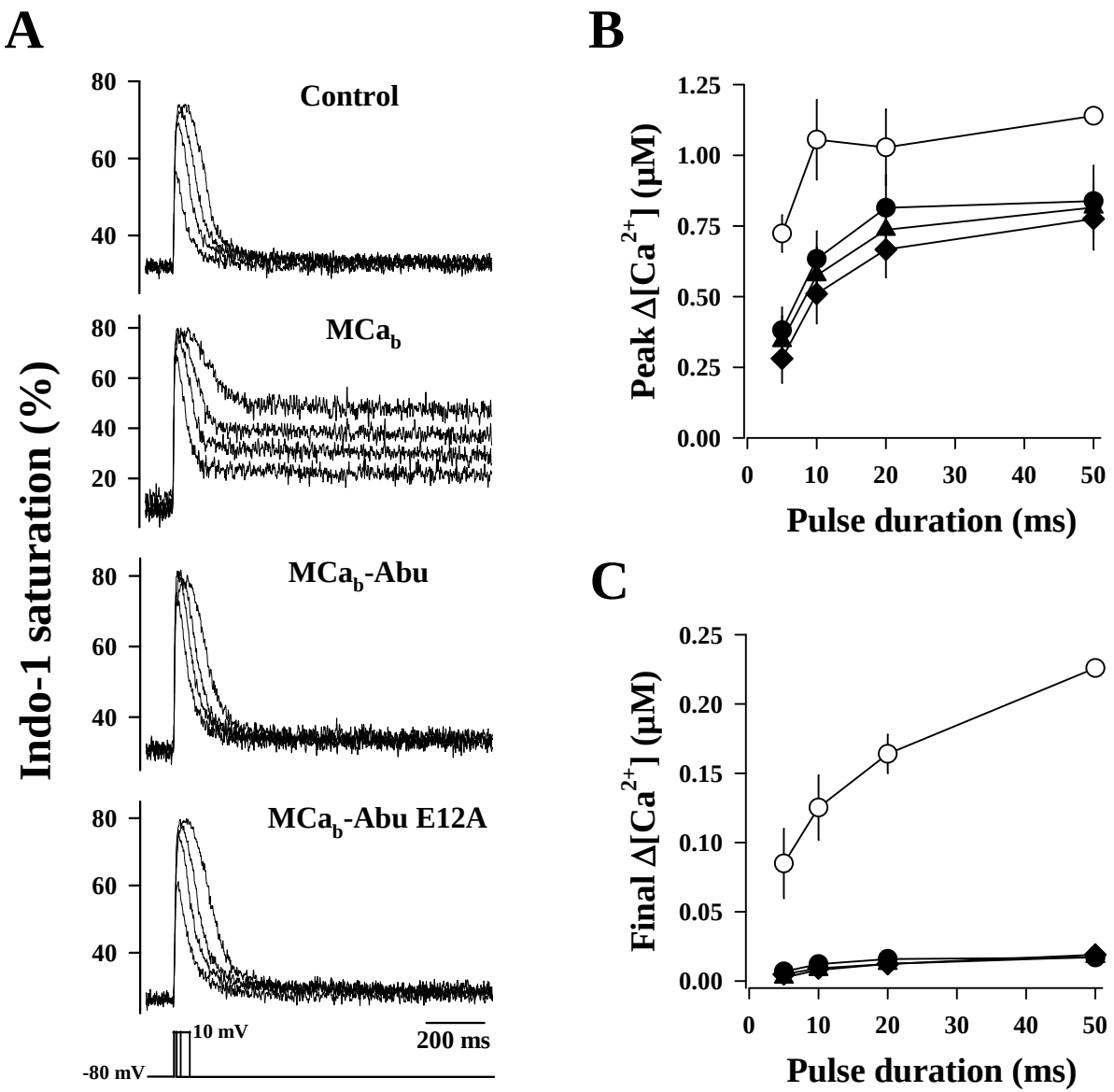

Figure 4 - Ram et al.

A

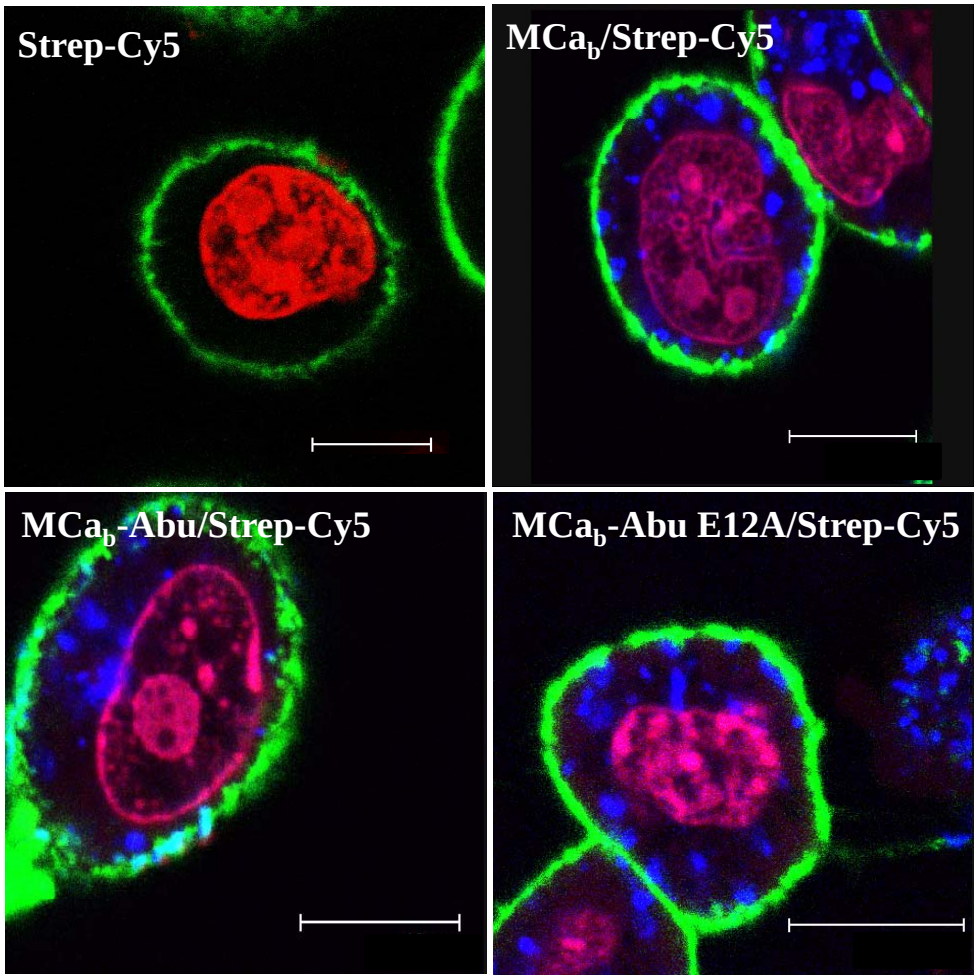

B

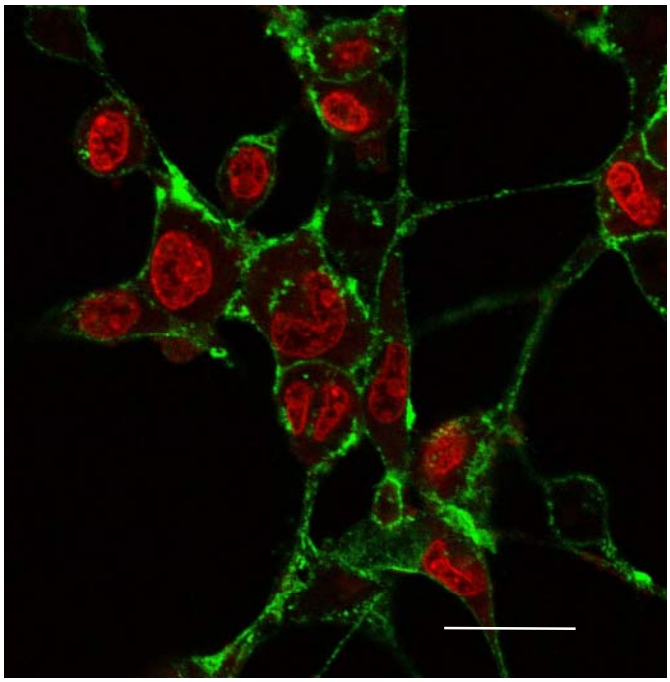

Figure 5 – Ram et al.

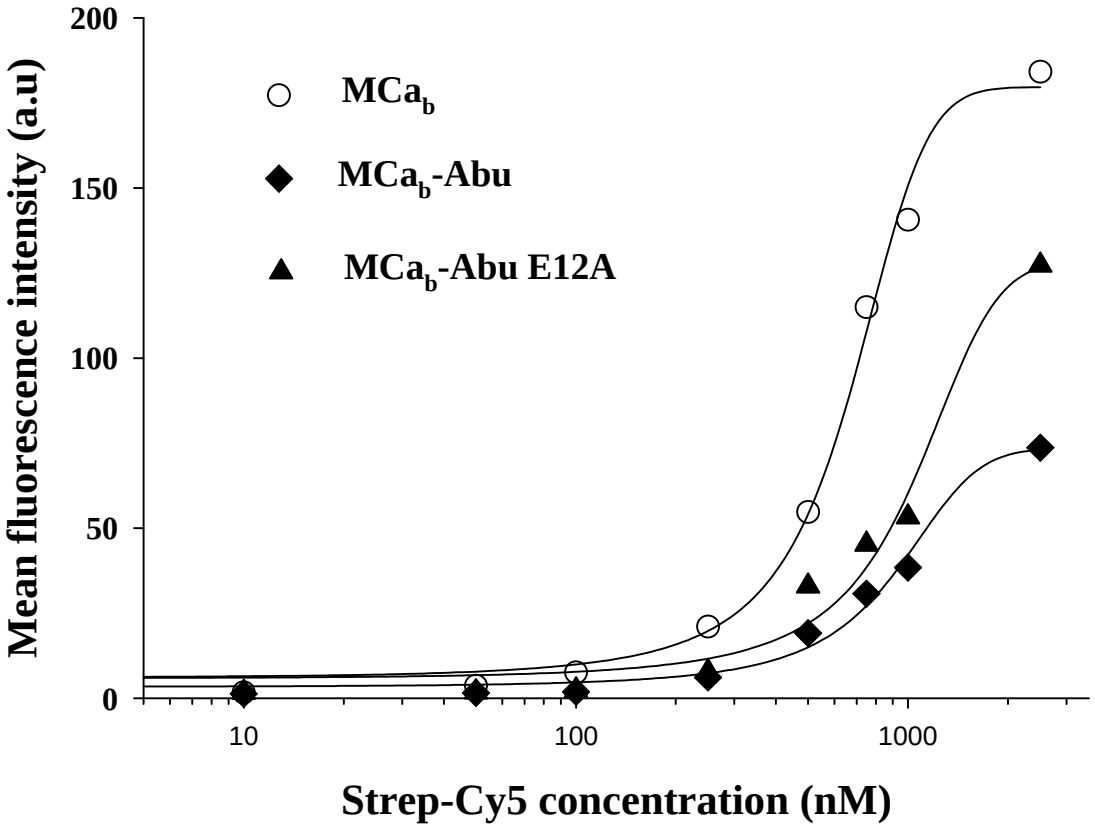

Figure 6 - Ram et al.

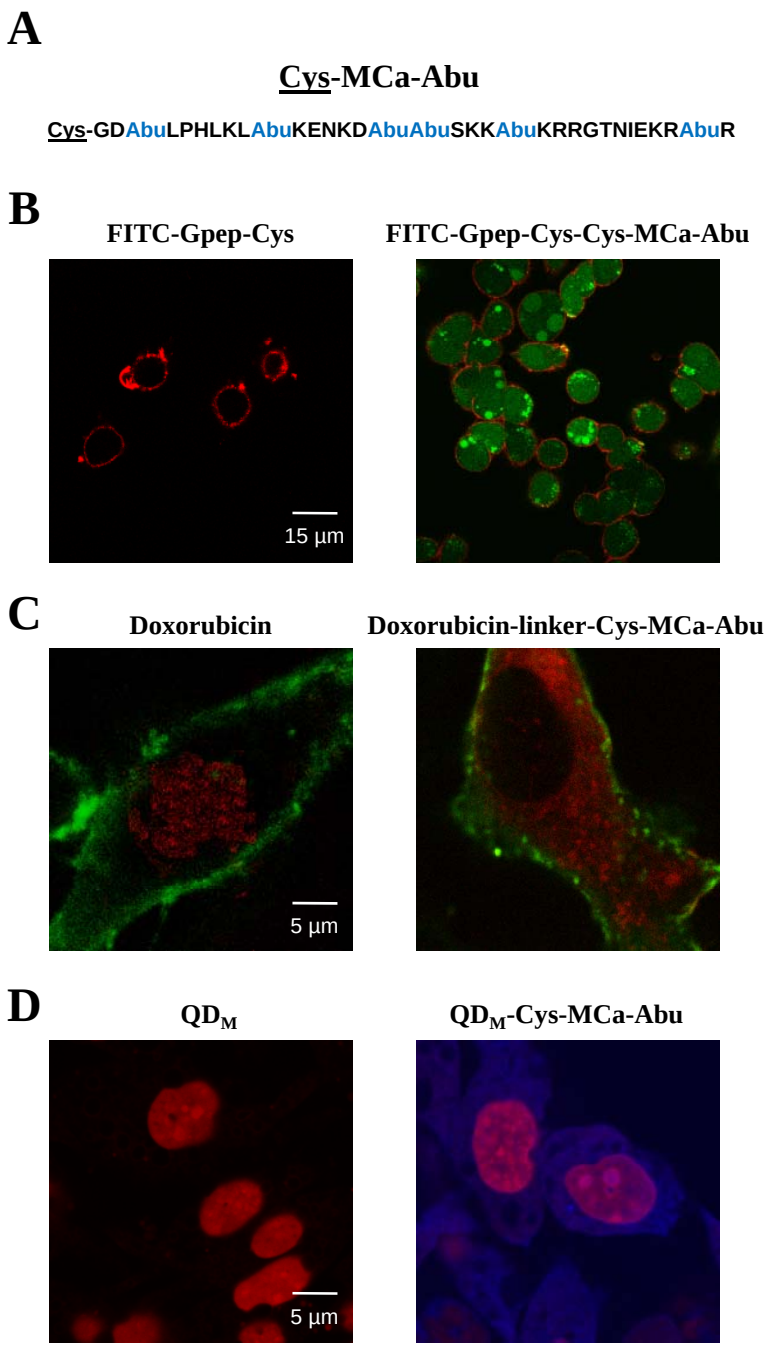

Figure 7 - Ram et al.

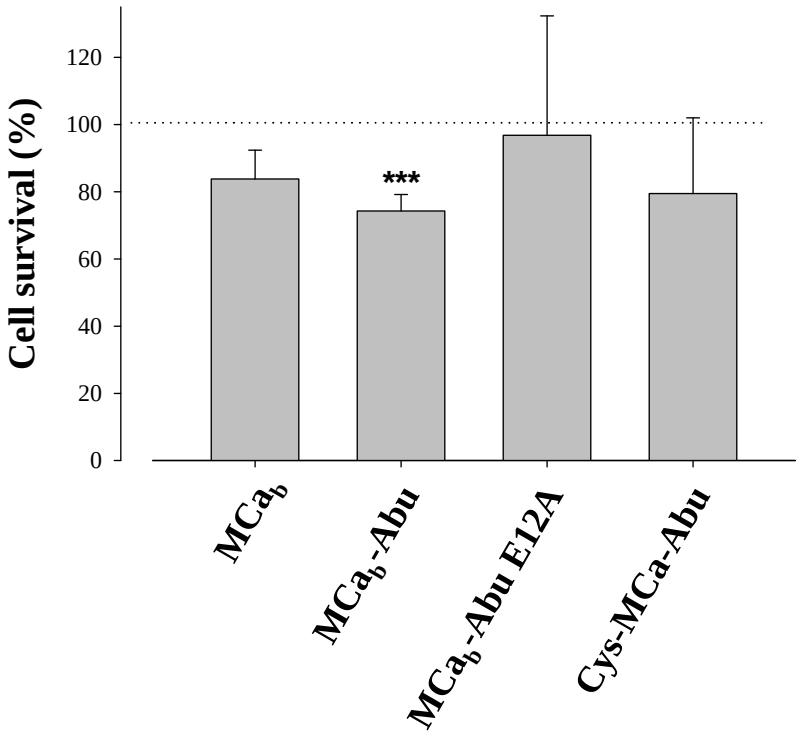

Figure 8 - Ram et al.